





# Brain Abnormalities in Patients with Germline Variants in *H3F3*: Novel Imaging Findings and Neurologic Symptoms Beyond Somatic Variants and Brain Tumors

 C.A.P.F. Alves, O. Sherbini, F. D'Arco,  D. Steel,  M.A. Kurian, F.C. Radio,  G.B. Ferrero,  D. Carli,  M. Tartaglia,  T.B. Balci, N.N. Powell-Hamilton, S.A. Schrier Vergano, H. Reutter,  J. Hoefele, R. Günthner,  E.R. Roeder,  R.O. Littlejohn,  D. Lessel,  S. Lüttgen,  C. Kentros,  K. Anyane-Yeboah,  C.B. Catarino,  S. Mercimek-Andrews,  J. Denecke,  M.J. Lyons,  T. Klopstock,  E.J. Bhoj,  L. Bryant, and  A. Vanderver



## ABSTRACT

**BACKGROUND AND PURPOSE:** Pathogenic somatic variants affecting the genes *Histone 3 Family 3A and 3B (H3F3)* are extensively linked to the process of oncogenesis, in particular related to central nervous system tumors in children. Recently, *H3F3* germline missense variants were described as the cause of a novel pediatric neurodevelopmental disorder. We aimed to investigate patterns of brain MR imaging of individuals carrying *H3F3* germline variants.

**MATERIALS AND METHODS:** In this retrospective study, we included individuals with proved *H3F3* causative genetic variants and available brain MR imaging scans. Clinical and demographic data were retrieved from available medical records. Molecular genetic testing results were classified using the American College of Medical Genetics criteria for variant curation. Brain MR imaging abnormalities were analyzed according to their location, signal intensity, and associated clinical symptoms. Numeric variables were described according to their distribution, with median and interquartile range.

**RESULTS:** Eighteen individuals (10 males, 56%) with *H3F3* germline variants were included. Thirteen of 18 individuals (72%) presented with a small posterior fossa. Six individuals (33%) presented with reduced size and an internal rotational appearance of the heads of the caudate nuclei along with an enlarged and squared appearance of the frontal horns of the lateral ventricles. Five individuals (28%) presented with dysgenesis of the splenium of the corpus callosum. Cortical developmental abnormalities were noted in 8 individuals (44%), with dysgyria and hypoplastic temporal poles being the most frequent presentation.

**CONCLUSIONS:** Imaging phenotypes in germline *H3F3*-affected individuals are related to brain features, including a small posterior fossa as well as dysgenesis of the corpus callosum, cortical developmental abnormalities, and deformity of lateral ventricles.

**H**istones are nuclear proteins that bind to DNA in the nucleus and help condense it into chromatin.<sup>1</sup> Histones are dynamically decorated with posttranslational modifications, which regulate the processes of DNA repair, gene expression, mitosis, and meiosis. Abnormal dysregulation of these posttranslational


modifications has been linked to cancer, neurodevelopmental syndromes, psychiatric disorders, and cardiovascular disease.<sup>2-5</sup> Therefore, histone biology is critical to understanding the pathophysiology of many diseases and developing treatments.

Received February 23, 2022; accepted after revision April 18.

From the Division of Neuroradiology (C.A.P.F.A.), Department of Radiology, Division of Human Genetics (E.J.B., L.B.), Department of Pediatrics, and Division of Neurology (A.V.), Department of Pediatrics, Children's Hospital of Philadelphia, Philadelphia, Pennsylvania; Department of Pediatrics, Children's Hospital of Philadelphia, Philadelphia, Pennsylvania; Departments of Radiology (F.D.) and Neurology (D.S., M.A.K.), Great Ormond Street Hospital for Children, London, UK; Molecular Neurosciences (D.S., M.A.K.), Zayed Centre for Research into Rare Diseases in Children, UCL GOS-Institute of Child Health, London, UK; Genetics and Rare Diseases Research Division (F.C.R., M.T.), Ospedale Pediatrico Bambino Gesù, IRCCS, Rome, Italy; Department of Public Health and Pediatrics (G.B.F., D.C.), University of Torino, Turin, Italy; Medical Genetics Program of Southwestern Ontario (T.B.B.), London Health Sciences Centre, London, Ontario, Canada; Department of Paediatrics (T.B.B.), Western University, London, Ontario, Canada; Division of Medical Genetics (N.N.P.-H.), Nemours Children's Hospital, Wilmington, Delaware; Division of Medical Genetics and Metabolism (S.A.S.V.), Children's Hospital of The King's Daughters, Norfolk, Virginia; Department of Pediatrics (S.A.S.V.), Eastern Virginia Medical School, Norfolk, Virginia; Division of Neonatology and Pediatric Intensive Care (H.R.), Department of Pediatrics and Adolescent Medicine, Friedrich-Alexander University Nürnberg-Erlangen, Erlangen, Germany; Institute of Human Genetics (J.H., R.G.) and Department of Nephrology (R.G.), Klinikum rechts der Isar, Technical University of Munich, School of Medicine, Munich, Germany; Department of Pediatrics and Molecular and Human Genetics (E.R.R., R.O.L.), Baylor College of Medicine, San Antonio,

Texas; Institute of Human Genetics (D.L., S.L.), University Medical Center Hamburg-Eppendorf, Hamburg, Germany; Division of Clinical Genetics (C.K., K.A.-Y.), Department of Pediatrics, Columbia University Vagelos College of Physicians and Surgeons and New York-Presbyterian, New York, New York; Friedrich-Baur-Institute (C.B.C., T.K.), Department of Neurology, University Hospital, Ludwig-Maximilian University Munich, Munich, Germany; German Center for Neurodegenerative Diseases (T.K.), Munich, Germany; Munich Cluster for Systems Neurology (T.K.), Munich, Germany; Department of Medical Genetics (S.M.-A.), Faculty of Medicine & Dentistry, University of Alberta, Edmonton, Alberta, Canada; Department of Medical Genetics (S.M.-A.), The Hospital for Sick Children, Toronto, Ontario, Canada; Department of Pediatrics (J.D.), University Medical Center Eppendorf, Hamburg, Germany; Greenwood Genetic Center (M.J.L.), Greenwood, South Carolina; and Department of Neurology (O.S., A.V.), Perelman School of Medicine, University of Pennsylvania, Philadelphia, Pennsylvania.

Please address correspondence to C.A. Alves, MD, PhD, Division of Neuroradiology, Department of Radiology, Children's Hospital of Philadelphia, 111 N 49th St, Philadelphia, PA 19139; e-mail: alvesc@chop.edu

 Indicates article with online supplemental data.

<http://dx.doi.org/10.3174/ajnr.A7555>

Pathogenic somatic variants affecting *H3F3* have been extensively linked to the epigenetic process of oncogenesis. In particular, when these variants involve 2 critical amino acids, p.Lys27 and p.Gly34, they are linked to central nervous system in children (p.Lys27 is linked to diffuse midline gliomas, and p.Gly34 is linked to supratentorial hemispheric gliomas).<sup>6-8</sup> Currently, these variants represent a major molecular feature for accurate classification of these neoplasms according to the World Health Organization.<sup>9</sup>

Expanding the correlation of this gene with human disease, Bryant et al<sup>10</sup> have recently demonstrated that *H3F3* plays a major role during embryogenesis, and causative pathogenic variants in these genes are associated with neurocognitive delay along with other symptoms such as seizures and hypotonia. In the present study, we sought to investigate the value of brain MR imaging in individuals carrying *H3F3A* or *H3F3B* germline variants, looking for an imaging pattern that would be recognizable for diagnostic purposes.

## MATERIALS AND METHODS

### Individual Population

This study included individuals with proved *H3F3* pathogenic and likely pathogenic variants that are causative of disease and with available clinical MR imaging scans of the brain. Individuals and their families were collected prospectively from the Myelin Disorders Bioregistry Project with approval from the institutional review board at Children's Hospital of Philadelphia (institutional review board approval No. IRB 14-011236). Written informed consent for the collection of clinical information, neuroimaging, and genetic information was obtained for each study participant.

### Abstraction of Clinical Data

Clinical and demographic data were retrieved from available medical records of affected individuals. Genetic testing reports were reviewed, or variants were provided by the referring provider and classified using the American College of Medical Genetics criteria for variant curation. All clinical and molecular data were reviewed by a board-certified clinical and/or clinical molecular geneticist.

### MR Imaging Technique

We retrospectively reviewed all available brain MR imaging studies of the included subjects. Images were acquired at either 1.5T or 3T MR using different imaging protocols including at least sagittal and axial T1WI and T2WI. MR images not allowing adequate visual assessment were excluded.

### Imaging Analysis

MR images of all individuals were reviewed independently by 2 pediatric neuroradiologists (C.A.P.F.A. and F.D.) with final consensus agreement in searching for structural features involving the posterior fossa, major commissural structures, and cortex, along with abnormalities in the ventricular system, basal ganglia, and thalamus. Additional evaluation, measurements, and ratios of the posterior fossa and corpus callosum, both evaluated in the sagittal midline, were performed to confirm the size abnormalities.<sup>11-15</sup> Detailed analysis of characteristics of white matter myelination was also performed.

**Table 1: Demographic, genetic, and clinical information of individuals with disease-causing missense variants<sup>a</sup>**

Characteristics	Individuals (n = 18)
Age at last evaluation (yr)	4.46 (1.9–12.1)
Sex: female/male	(8:10)
<i>H3F3</i> variant	
<i>H3F3A</i>	11 (61)
<i>H3F3B</i>	7 (39)
Microcephaly	8 (44)
Seizures	10 (56)
Febrile	5 (50)
Nonfebrile	5 (50)
Sitting (n = 17)	
Normal	1 (6)
Delayed	12 (71)
Not achieved	4 (23)
Walking	
Normal	2 (11)
Delayed	10 (56)
Not achieved	6 (33)
Speaking	
Normal	1 (6)
Delayed	7 (38)
Not achieved	10 (56)

<sup>a</sup>Categoric variables are described as number (percentage). Continuous variables are described as median (IQ–3Q).

### Statistical Analysis

Statistical analyses were performed using R statistical and computing software (<http://www.r-project.org>) and R studio (<http://rstudio.org/download/desktop>). A 2-tailed  $P < .05$  was considered statistically significant. The Shapiro-Wilk test was used to assess the normality of continuous variables, which were presented as median and first and third quartiles (1Q–3Q). Categoric variables were presented as counts and percentages. Mann-Whitney *U* or Student *t* tests were used to compare continuous variables, and the Fisher exact test was used to compare categoric variables between clinical data and MR imaging findings. For statistical analysis, individuals were divided into 2 groups, nonachievement milestones versus normal achievement plus development delay. Delayed and normal developmental milestones were grouped together due to the small number of subjects with normal development. Delayed milestones were defined as sitting after 6 months, walking after 20 months, and first word after 12 months of age.

## RESULTS

On the basis of the inclusion criteria, a cohort of 18 individuals (mean age, 4.5 years; range, 1.9–12.1 years; 10 males/8 females) with proved *H3F3* variants causative of disease were included in this study. All individuals underwent brain MR imaging. These individuals had 1 of 2 genotypes: *H3F3A* variants ( $n = 11$ ) or *H3F3B* variants ( $n = 7$ ). The details of each individual's demographic, clinical, and genetic information are given in Table 1 and the Online Supplemental Data. The overall imaging findings are described in Table 2.

### Posterior Fossa

Thirteen of 18 individuals (72%) presented with a verticalized tentorium and low insertion of the torcula, along with features

**Table 2: Abnormal imaging information of individuals with disease-causing H3F3 missense variants<sup>a</sup>**

Imaging Features	Individuals (n = 18)
Small posterior fossa	13 (72)
Cerebellum	2 (11)
Brainstem	2 (11)
Thalamus	0
Caudate	8 (44)
Putamen	0
Globus pallidum	0
Corpus callosum	5 (28)
Fourth ventricle	6 (33)
Lateral ventricle	7 (38)
White matter	2
Cortex	8 (44)
Optic nerves and chiasm	1 (6)
Temporal lobes/hippocampus	8 (44)
Clivus/sella	4 (22)

<sup>a</sup> Categorical variables are described as number (percentage).

suggestive of a small posterior fossa and hypoplasia of the occipital bone, later confirmed with additional posterior fossa measurements and ratios (Online Supplemental Data).<sup>13-15</sup> The occipital bone, measured by the supraoccipital line, of those patients with a small posterior fossa was disproportionately small, and it was significantly smaller ( $P = .001$ ) compared with the subjects with a normal posterior fossa. Of those, 7 individuals (7/13 54%) had posterior fossa structures (brainstem and cerebellum) that appeared crowded (Fig 1A–D). A low disposition of the cerebellar tonsils fitting in the Chiari I deformity criteria<sup>15</sup> was observed in 4

individuals. Further mild malformative features of the brainstem were observed in 2 children: both with abnormal anterior-posterior pattern of malformations, one with disproportional predominance of the midbrain (Online Supplemental Data) and the other with disproportional size reduction of the midbrain compared with the medulla oblongata (Online Supplemental Data). Hypoplasia of the clivus and signs of platybasia were noted in 3 individuals.

### Major Commissures

Malformative features of the corpus callosum, accompanied or not accompanied by anterior commissure hypoplasia, were present in 5 individuals (28%). The involvement of the splenium of the corpus callosum was the most remarkable feature, being absent or elongated and hypoplastic according to the patient's age in all 5 cases. Agenesis of the body and splenium of the corpus callosum was observed in 1 case (5.5%) (Fig 1A–D and Online Supplemental Data).

### Cortex

The cerebral cortex of 8 individuals (44%) presented with malformative features. Six of them showed variable degrees of diffuse dysgyria, (Fig 2A–D) 1 anterior pachygyria, and 1 diffuse simplified cortical appearance. Along with the cortical abnormalities, all 8 individuals also had bilateral temporal lobe hypoplasia (Fig 2E–H).

### Basal Ganglia and Lateral Ventricles

Six individuals (33%) presented with a relatively reduced size and/or internal rotational appearance of the heads of the caudate nuclei. These features resulted in a characteristic deformity of the lateral

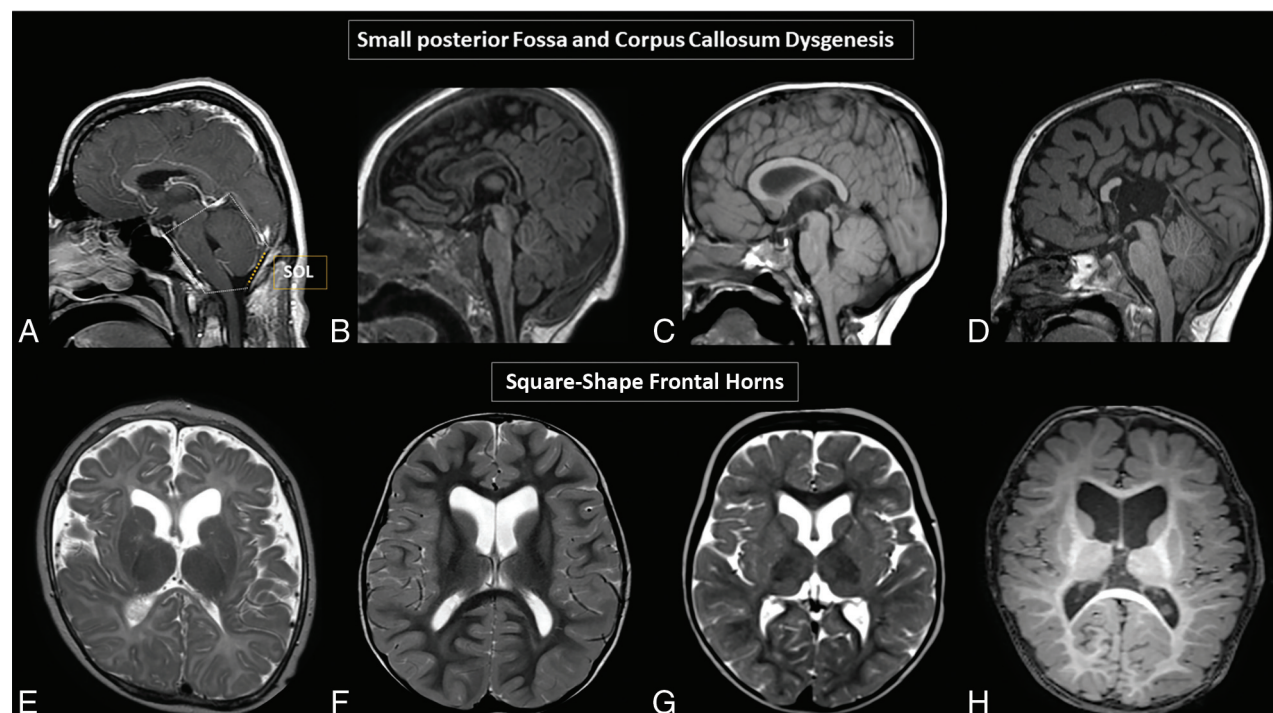


**FIG 1.** Brain MR images. A and D, Variable degrees of corpus callosum deformities, particularly involving the body and splenium, noting partial agenesis in D. Deformed morphology of the posterior fossa, with variable degrees of low insertion of the torcula and size reduction of the supraoccipital line (SOL). Note the crowded appearance of the structures in the posterior fossa along with low disposition of the cerebellar tonsils, fitting in the Chiari I deformity criteria in C and D. E–H, Variable degrees of reduced size and/or internal rotational appearance of the head of the caudate nuclei, resulting in an enlarged and squared appearance of the frontal horns.

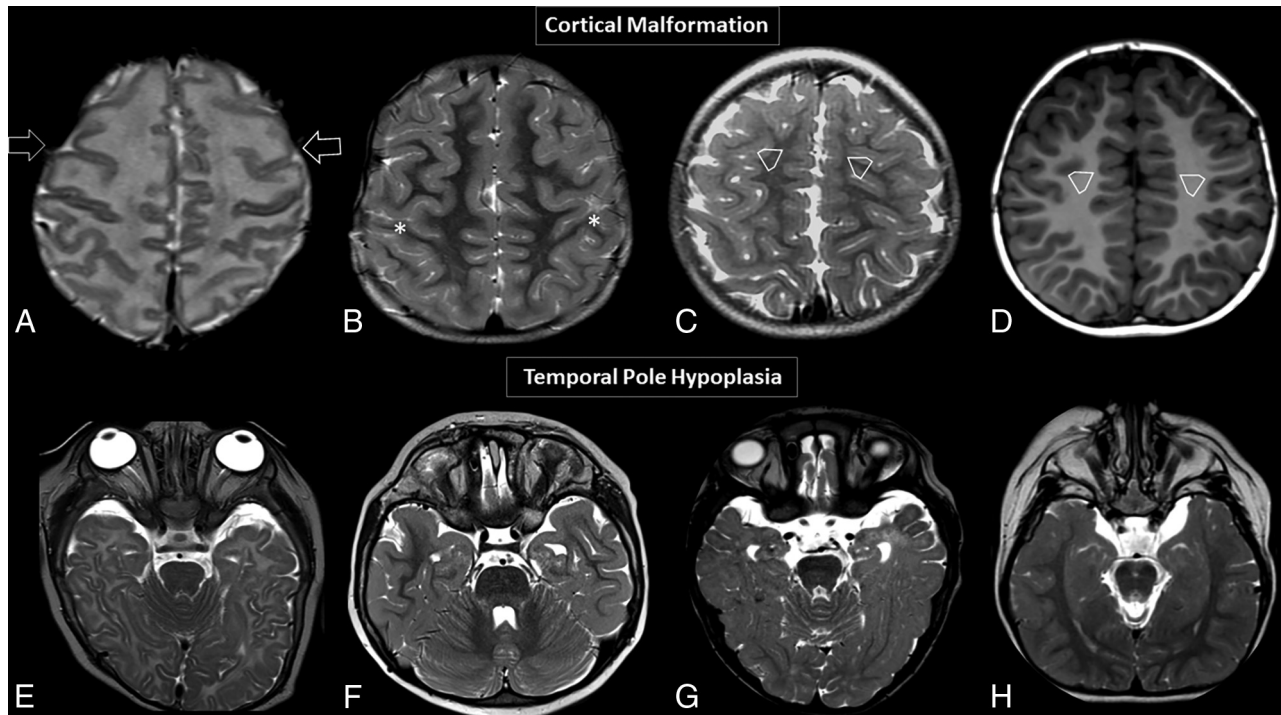


**FIG 2.** Brain MR images. Axial T2WI (A–C) and axial T1WI (D) showing 4 different patients with variable degrees of diffuse abnormal orientation and morphology of the gyri and sulci. Note particular abnormal morphology involving both frontal lobes (*open arrows*, A), a deformed periorbital region (*asterisks*, B), and abnormal gyration of the medial frontal lobes in C and D (*open arrowheads*, C and D). Axial T2WI (E–H) shows 4 different patients with temporal pole hypoplasia.

ventricles, with an enlarged and squared appearance of the frontal horns (Fig 1E–H).

### Clinical Correlation

Our entire cohort ( $n = 18$ ) presented with at least 1 clinical symptom, including microcephaly, the presence of seizures, and delayed or not delayed achieved development milestones (Table 1).

No statistically significant ( $P < .05$ ) correlation between clinical symptoms (absence of achievement of gross motor and speaking milestones, presence of seizures) and main imaging findings (small posterior fossa, basal ganglia abnormalities, and corpus callosum and cortical malformations) was found. However, all individuals included in our cohort except for 1 had severe clinical symptoms and marked abnormalities involving the brain. Moreover, 50% of individuals presenting with seizures also had malformative features involving the cortex (Online Supplemental Data).

### DISCUSSION

Somatic variants in *H3F3* are well-known promoters of oncogenesis;<sup>16–19</sup> however, the role of germline variants remain underrecognized. The recent discovery of disease-associated missense variants in *H3F3* that cause a neurodevelopmental disorder, but not cancer, profoundly impacts histone biology research.<sup>10</sup> In the present study, we sought to investigate the value of brain MR imaging of individuals carrying *H3F3* germline variants, assessing imaging patterns and the neurodegenerative clinical symptoms. We found a constellation of malformative features of the brain, including a small posterior fossa, along with changes in the basal ganglia, cortex, and corpus callosum.

Neuroimaging plays an important role in the diagnosis of pediatric glial tumors related to pathogenic somatic variants affecting *Histone 3 Family 3A and 3B*.<sup>9,16,20–22</sup> Because some recent studies have demonstrated the critical importance of histone turnover in neuronal transcription and plasticity in the mammalian brain<sup>23–25</sup> and Bryant et al<sup>10</sup> have demonstrated the role of germline variants of *H3F3* during embryogenesis as a causative factor of neurocognitive delay in young individuals, we have investigated the potential presentation of malformative features in the brain MR imaging of these individuals and how these would impact the patient's prognosis.

Individuals with disease-causing germline variants in histone 3.3 in our cohort had a characteristic clinical background, usually presenting with neurocognitive delay, seizures, and microcephaly. On neuroimaging, our cohort also shared some similar features; the most prevalent was a small posterior fossa (13/18 individuals), with some of them presenting with Chiari I deformity and malformative features affecting the brainstem or cerebellum. There is a wide spectrum of congenital abnormalities associated with a small posterior fossa, including developmental malformations caused by a genetic defect<sup>26–28</sup> as well as disruptive causes due to injury of a structure with normal developmental potential.<sup>29–32</sup> Understanding the spectrum of congenital posterior fossa anomalies and their diagnostic criteria is of paramount importance for optimal therapy, accurate prognosis, and correct genetic counseling.<sup>29</sup>

We have encountered further neuroimaging findings in our cohort of individuals with disease-causing germline missense variants in *H3F3*. The findings included enlarged frontal horns of the lateral ventricles, reflecting reduced size and/or an internal

rotational appearance of the nuclei of the caudate heads, dysgenesis of the corpus callosum, and malformations of cortical development, such as dysgyria. Cortical malformation implies abnormalities in both the migration of neurons to the cortex and abnormal cortical organization<sup>33,34</sup> and may underlie the relatively high frequency of epilepsy in those individuals.<sup>35,36</sup>

No statistical significance ( $P < .05$ ) was found correlating milestones delay (in sitting, walking, and speaking the first word) or the presence of seizures with the main imaging findings, including a small posterior fossa, basal ganglia abnormalities, and corpus callosum and cortical malformations. Fifty percent of individuals presenting with seizures also had malformative features involving the cortex, suggesting a potential correlation between both.

Despite presenting promising findings, our study also had limitations, including the retrospective nature of our study design. Our cohort was biased because all individuals included in our study except for 1 had severe clinical symptoms and significant abnormalities involving the brain, making correlative analysis more difficult. The other limitation was that we had a relatively small sample size of individuals who had brain MR imaging assessment, though it represents almost half of the 43 reported individuals in the literature. On the other hand, we found consistent neuroimaging findings among our cohort, which is helpful for guiding appropriate genetic investigations of these individuals. Our imaging findings may reflect the spectrum of abnormalities seen in individuals with germline variants in histone 3.3; however, these results need to be validated in a larger cohort with broader disease severity.

## CONCLUSIONS

The current series, including a subset of individuals previously reported in the original work of Bryant et al,<sup>10</sup> represents the largest cohort of neuroradiologically characterized subjects carrying disease-causing *H3F3* germline variants. The identified constellation of neuroimaging findings, namely a small posterior fossa, reduced size and/or a rotational appearance of the nuclei of the caudate heads, dysgenesis of the corpus callosum, and malformations of cortical development, offer novel diagnostic pattern able to guide the diagnosis of *H3F3*-related disorder.

## ACKNOWLEDGMENTS

We are grateful to the patients and their families for their involvement in this study. We also thank Lydia Sheldon, MSED, for helpful editing suggestions.

Disclosure forms provided by the authors are available with the full text and PDF of this article at [www.ajnr.org](http://www.ajnr.org).

## REFERENCES

- Mariño-Ramírez L, Kann MG, Shoemaker BA, et al. **Histone structure and nucleosome stability.** *Expert Rev Proteomics* 2005;2:719–29 [CrossRef Medline](#)
- Zhao Z, Shilatifard A. **Epigenetic modifications of histones in cancer.** *Genome Biol* 2019;20:245 [CrossRef Medline](#)
- Kim JH, Lee JH, Lee IS, et al. **Histone lysine methylation and neurodevelopmental disorders.** *Int J Mol Sci* 2017;18:1404 [CrossRef Medline](#)
- Peter CJ, Akbarian S. **Balancing histone methylation activities in psychiatric disorders.** *Trends Mol Med* 2011;17:372–79 [CrossRef Medline](#)
- Bagchi RA, Weeks KL. **Histone deacetylases in cardiovascular and metabolic diseases.** *J Mol Cell Cardiol* 2019;130:151–59 [CrossRef Medline](#)
- Sturm D, Witt H, Hovestadt V, et al. **Hotspot mutations in H3F3A and IDH1 define distinct epigenetic and biological subgroups of glioblastoma.** *Cancer Cell* 2012;22:425–37 [CrossRef Medline](#)
- Aboian MS, Solomon DA, Felton E, et al. **Imaging characteristics of pediatric diffuse midline gliomas with histone H3 K27M mutation.** *AJNR Am J Neuroradiol* 2017;38:795–800 [CrossRef Medline](#)
- Kurokawa R, Baba A, Kurokawa M, et al. **Neuroimaging features of diffuse hemispheric glioma, H3 G34-mutant: a case series and systematic review.** *J Neuroimaging* 2022;32:17–27 [CrossRef Medline](#)
- Louis DN, Perry A, Wesseling P, et al. **The 2021 WHO Classification of Tumors of the Central Nervous System: a summary.** *Neuro Oncol* 2021;23:1231–51 [CrossRef Medline](#)
- Bryant L, Li D, Cox SG, et al. **Histone H3.3 beyond cancer: germline mutations in Histone 3 Family 3A and 3B cause a previously unidentified neurodegenerative disorder in 46 patients.** *Sci Adv* 2020;6:eabc9207 [CrossRef Medline](#)
- Garel C, Cont I, Alberti C, et al. **Biometry of the corpus callosum in children: MR imaging reference data.** *AJNR Am J Neuroradiol* 2011;32:1436–43 [CrossRef Medline](#)
- Jandeaux C, Kuchcinski G, TERNYNCK C, et al. **Biometry of the cerebellar vermis and brain stem in children: MR imaging reference data from measurements in 718 children.** *AJNR Am J Neuroradiol* 2019;40:1835–41 [CrossRef Medline](#)
- Marin-Padilla M, Marin-Padilla TM. **Morphogenesis of experimentally induced Arnold–Chiari malformation.** *J Neurol Sci* 1981;50:29–55 [CrossRef Medline](#)
- Nishikawa M, Sakamoto H, Hakuba A, et al. **Pathogenesis of Chiari malformation: a morphometric study of the posterior cranial fossa.** *J Neurosurg* 1997;86:40–47 [CrossRef Medline](#)
- Poretti A, Ashmawy R, Garzon-Muvdi T, et al. **Chiari type 1 deformity in children: pathogenetic, clinical, neuroimaging, and management aspects.** *Neuropediatrics* 2016;47:293–307 [CrossRef Medline](#)
- Schwartzentruber J, Korshunov A, Liu XY, et al. **Driver mutations in histone H3.3 and chromatin remodelling genes in paediatric glioblastoma.** *Nature* 2012;482:226–31 [CrossRef Medline](#)
- Weinberg DN, Allis CD, Lu C. **Oncogenic mechanisms of histone H3 mutations.** *Cold Spring Harb Perspect Med* 2017;7:a026443 [CrossRef Medline](#)
- Khuong-Quang DA, Buczkowicz P, Rakopoulos P, et al. **K27M mutation in histone H3.3 defines clinically and biologically distinct subgroups of pediatric diffuse intrinsic pontine gliomas.** *Acta Neuropathol* 2012;124:439–47 [CrossRef Medline](#)
- Feng J, Hao S, Pan C, et al. **The H3.3 K27M mutation results in a poorer prognosis in brainstem gliomas than thalamic gliomas in adults.** *Hum Pathol* 2015;46:1626–32 [CrossRef Medline](#)
- Castel D, Philippe C, Calmon R, et al. **Histone H3F3A and HIST1H3B K27M mutations define two subgroups of diffuse intrinsic pontine gliomas with different prognosis and phenotypes.** *Acta Neuropathol* 2015;130:815–27 [CrossRef Medline](#)
- Aboian MS, Tong E, Solomon DA, et al. **Diffusion characteristics of pediatric diffuse midline gliomas with histone H3-K27M mutation using apparent diffusion coefficient histogram analysis.** *AJNR Am J Neuroradiol* 2019;40:1804–10 [CrossRef Medline](#)
- Piccardo A, Tortora D, Mascelli S, et al. **Advanced MR imaging and 18F-DOPA PET characteristics of H3K27M-mutant and wild-type pediatric diffuse midline gliomas.** *Eur J Nucl Med Mol Imaging* 2019;46:1685–94 [CrossRef Medline](#)
- Maze I, Wenderski W, Noh K-M, et al. **Critical role of histone turnover in neuronal transcription and plasticity.** *Neuron* 2015;87:77–94 [CrossRef Medline](#)
- Deal RB, Henikoff JG, Henikoff S. **Genome-wide kinetics of nucleosome turnover determined by metabolic labeling of histones.** *Science* 2010;328:1161–64 [CrossRef Medline](#)
- Dion MF, Kaplan T, Kim M, et al. **Dynamics of replication-independent histone turnover in budding yeast.** *Science* 2007;315:1405–08 [CrossRef Medline](#)

26. Hennekam RC, Biesecker LG, Allanson JE, et al; Elements of Morphology Consortium. **Elements of morphology: general terms for congenital anomalies.** *Am J Med Genet A* 2013;161A:2726–33 [CrossRef Medline](#)
27. Doherty D, Millen KJ, Barkovich AJ. **Midbrain and hindbrain malformations: advances in clinical diagnosis, imaging, and genetics.** *Lancet Neurol* 2013;12:381–93 [CrossRef Medline](#)
28. Boycott KM, Flavelle S, Bureau A, et al. **Homozygous deletion of the very low density lipoprotein receptor gene causes autosomal recessive cerebellar hypoplasia with cerebral gyral simplification.** *Am J Hum Genet* 2005;77:477–83 [CrossRef Medline](#)
29. Bosemani T, Orman G, Boltshauser E, et al. **Congenital abnormalities of the posterior fossa.** *Radiographics* 2015;35:200–20 [CrossRef Medline](#)
30. Limperopoulos C, Soul JS, Gauvreau K, et al. **Late gestation cerebellar growth is rapid and impeded by premature birth.** *Pediatrics* 2005;115:688–95 [CrossRef Medline](#)
31. Messerschmidt A, Prayer D, Brugger PC, et al. **Preterm birth and disruptive cerebellar development: assessment of perinatal risk factors.** *Eur J Paediatr Neurol* 2008;12:455–60 [CrossRef Medline](#)
32. Steggerda SJ, Leijser LM, Wiggers-de Bruïne FT, et al. **Cerebellar injury in preterm infants: incidence and findings on US and MR images.** *Radiology* 2009;252:190–99 [CrossRef Medline](#)
33. Barkovich AJ, Kuzniecky RI, Jackson GD, et al. **Classification system for malformations of cortical development: update 2001.** *Neurology* 2001;57:2168–78 [CrossRef Medline](#)
34. Barkovich AJ, Kuzniecky RI, Jackson GD, et al. **A developmental and genetic classification for malformations of cortical development.** *Neurology* 2005;65:1873–87 [CrossRef Medline](#)
35. Shorvon S, Guerrini R, Trinka E, et al. *The Causes of Epilepsy: Diagnosis and Investigation.* Cambridge University Press; 2019
36. Barkovich AJ, Guerrini R, Kuzniecky RI, et al. **A developmental and genetic classification for malformations of cortical development: update 2012.** *Brain* 2012;135:1348–69 [CrossRef Medline](#)